—Regular Article—

Formulation Optimization and Characterization of Spray Dried Microparticles for Inhalation Delivery of Doxycycline Hyclate

Madhusmita MISHRA and Brahmeshwar MISHRA*

Department of Pharmaceutics, Institute of Technology, Banaras Hindu University, Varanasi-221005, India

(Received July 20, 2011; Accepted September 26, 2011)

The local delivery of antibiotics in the treatment of infectious respiratory diseases is an attractive alternative to deliver high concentration of antimicrobials directly to the lungs and minimize systemic side effects. In this study, inhalable microparticles containing doxycycline hyclate, sodium carboxymethylcellulose, leucine and lactose were prepared by spray drying of aqueous ethanol formulations. Box-Behnken design was used to study the influence of various independent variables such as polymer concentration, leucine concentration, ethanol concentration and inlet temperature of the spray dryer on microparticle characteristics. The microparticles were characterized in terms of particle morphology, drug excipient interaction, yield, entrapment efficiency, Carr's index, moisture content, thermal properties, X-ray powder diffraction, aerosolization performance and *in vitro* drug release. The effect of independent variables on spray dryer outlet temperature was also studied. The overall shape of the particles was found to be spherical like doughnuts in the size range of 1.16–5.2 μm. The optimized formulation (sodium carboxymethylcellulose concentration 14% w/v, leucine concentration 33% w/v, ethanol concentration 36% v/v, inlet temperature of 140°C) exhibited the following properties: yield 56.69%, moisture content 3.86%, encapsulation efficiency 61.74%, theoretical aerodynamic diameter 3.11 μm and Carr's index 23.5% at an outlet temperature 77°C. The powders generated were of a suitable mass median aerodynamic diameter (4.89 μm) with 49.3% fine particle fraction and exhibited a sustained drug release profile *in vitro*.

Key words——antibiotic; inhalable microparticle; spray drying; Box-Behnken design

INTRODUCTION

Inhalation delivery of antibiotics is an attractive therapeutic option in the treatment of infectious respiratory diseases. The pulmonary drug concentration achievable by either oral or parenteral administration is much lower than that obtained by inhalation route.[1] Local delivery of drug is expected to reduce the therapeutic dose, minimize side effects and decrease the need for parenteral therapy, especially in hospitalised patients. Researchers are now focussing on the development of colloidal drug carriers such as microparticles in the size range of 1–5 μm for deposition in the lung. These systems are expected to enhance patient convenience and compliance by modifying drug release or improving local drug retention. Microparticles in this size range exhibit strong interparticulate cohesion, leading to poor powder flow properties. Different particle engineering approaches have been employed by various researchers to tailor the need of desired aerosolisation properties (e.g., particle morphology, density and surface characteristics) in the final product. This includes manipulation of percentage of fines and surface rugosity,[2] addition of ternary agents,[3] design of elongated particle,[4] addition of force controlling agents[5] or addition of hygroscopic growth inhibitors.[6]

Spray drying is a unique single step constructive method for microencapsulation of drug in polymeric carriers. Spray drying involves the transformation of a material from a fluid state into a dried particulate form by spraying the atomized feed into a hot drying gas (mostly air) medium. Adjustment of many parameters such as temperature of inlet air, rate of liquid feed entry, atomizing pressure and total solid content of feed or feed viscosity provides greater control over particle size, shape and density. This method is highly reproducible, relatively easy to scale up, offers a narrow particle size distribution and also ensures dose uniformity even when the drug dose is very low. However, the spray drying process variables must be controlled to avoid low yields, sticking and high moisture content. Spray dried particulates can be designed by inclusion of polymers such as, hyaluronan,[7] polylactic acid,[8] chitosan,[9] and poly(lactic-co-glycolic acid).[10] Among the cellulose based poly-

*e-mail: bmishrabhu@rediffmail.com

mers, hydroxypropyl cellulose[11] and hydroxypropyl methyl cellulose[12] have been studied for inhalation delivery. Recently, suspension of spray dried sodium carboxymethyl cellulose (SC) powder was found to be a promising alternative in the pressurized metered dose inhalation delivery of bovine serum albumin.[13] It is a hydrophilic polysaccharide characterised by low toxicity and high biocompatibility for alveolar cells.[14] SC carrier also has mucoadhesive properties related to the open expanded conformation in the hydrated state and presence of solubilized carboxylic acid groups available for hydrogen bonding to mucin glycoproteins.[15] In the present work, inhalable SC based microparticles of doxycycline hyclate (DX) were prepared by spray drying. DX is a broad spectrum antimicrobial[16] effective against a wide variety of bacteria, such as *Hemophilus influenzae*, *Streptococcus pneumonia* and *Mycoplasma pneumonia*. A significant advantage of DX is its activity against tetracycline-resistant *S. aureus*. Recently, its activity against matrix metalloproteinase[17] has found application in the reduction of inflammatory changes associated with cystic fibrosis and chronic lung diseases.

The aim of this study was to optimize the feed composition and process parameter in spray drying using a Box-Behnken design. This technique is an independent, rotatable or nearly rotatable modified central composite experimental design. The combinations of variables are at the midpoints of the edges of the process space and at the center.[18] This method is advantageous over other response surface methodologies as it avoids combination of extreme factors. Also, it does not contain combinations for which all factors are simultaneously at their highest or lowest levels. Experiments performed under extreme conditions are usually unacceptable. The second order polynomial equation generated by this experimental design is as follows:

$$Y_i = b_0 + b_1X_1 + b_2X_2 + b_3X_3 + b_4X_4 + b_{12}X_1X_2 + b_{13}X_1X_3 + b_{14}X_1X_4 + b_{23}X_2X_3 + b_{24}X_2X_4 + b_{34}X_3X_4 + b_{11}X_1^2 + b_{22}X_2^2 + b_{33}X_3^2 + b_{44}X_4^2 \quad (1)$$

where Y_i is the dependent variable, b_0 is the intercept, b_1 to b_{44} are the regression coefficients, and X_1, X_2, X_3 and X_4 are the independent variables selected from preliminary experiments.

MATERIALS AND METHODS

Materials DX was obtained as a gift sample from Ranbaxy Laboratories Ltd. (Gurgaon, India). Sodium carboxymethylcellulose (SC, 1500–3000 cps) was purchased from Sigma - Aldrich India Ltd, (New Delhi, India). All other chemicals used were of analytical reagent grade and obtained from Qualigens Fine Chemicals (Mumbai, India).

Methods

Preparation of Spray Dried Microparticles

Microparticles containing DX, polymer (SC), leucine and lactose were prepared by spray drying. In each batch, DX was first dissolved in the aqueous polymeric solution. This was followed by addition of leucine and lactose. Stirring was continued until a clear solution was obtained on addition of ethanol. 250 ml of the prepared formulation was then spray dried using a laboratory spray drier (Jay Instruments and Systems Pvt. Ltd., LSD-48, India). The feed was sprayed through a 0.7 mm two fluid nozzle at the rate of 3 ml/min by a peristaltic pump. In all the experiments, drying air rate was kept constant at 28 m^3/h. The spray dried powders were collected from the product collection chamber. Material adhering to the chamber lid as well as lower portion of the cyclone chamber taper was collected using a brush.

Experimental Design In the present study, a three level four factorial Box-Behnken experimental design was used. The quadratic response surfaces and second order polynomial models were generated using Minitab 16 software (Minitab Ltd., Coventry, UK). A total of 27 experimental runs with three replications of the central point are shown in Table 1. By means of this experimental design, the effect of four factors namely, polymer (SC) concentration, leucine (dispersibility enhancer) concentration, ethanol concentration and inlet temperature was studied on product characteristics. All runs of the experiment were performed in a randomised manner to eliminate any unknown possible sources of bias. Each batch was prepared in duplicate and evaluated in terms of yield, moisture content, entrapment efficiency and aerodynamic diameter.

In order to describe quantitatively how the various input variables affected the responses in our system, an empirical statistical model was constructed. The model is the linear best-fit equation describing the response as the sum of an intercept and the product of the inputs and their fitted parameter estimates. A positive parameter indicates that the response increases with increasing input variables. Conversely,

Table 1. Run Variables and Response Values of the Four Factor, Three Level Box-Behnken Design

Run order	Polymer conc. (% w/v)	Leucine conc. (% w/v)	Ethanol (% v/v)	Inlet temp. (℃)	Yield (%)	Moisture content (%)	EE (%)	CI (%)	d_{aero} (μm)	Outlet temp. (℃)
1	10	24	65	140	32.44	3.00	66.70	34.8	2.60	78.0
2	10	36	65	140	37.40	3.00	68.05	27.8	2.80	75.0
3	5	30	35	140	24.34	2.00	51.80	28.5	1.60	73.0
4	10	24	35	140	36.72	3.28	64.20	34.8	2.30	79.0
5	10	36	50	120	42.30	4.00	64.42	30	1.87	67.0
6	10	36	35	140	42.62	3.35	62.00	27.8	2.48	82.0
7	5	30	50	160	25.22	1.49	59.00	25.6	1.98	97.0
8	10	36	50	160	40.16	1.48	68.87	22.4	2.37	87.9
9	5	24	50	140	20.62	2.20	55.53	40.8	1.34	73.0
10	15	30	50	120	52.32	4.50	65.60	29.8	5.00	64.8
11	15	30	50	160	54.2	2.50	67.90	15.6	4.30	88.0
12	10	30	65	120	37.43	3.50	67.71	28.6	3.06	64.8
13	10	30	65	160	32.86	1.59	68.03	21.2	2.77	87.9
14	10	24	50	120	34.31	3.50	66.02	36.8	3.24	67.0
15	10	30	50	140	37.82	3.10	64.56	22.8	2.70	82.0
16	10	30	35	120	38.42	3.80	60.05	26.8	3.00	57.0
17	10	24	50	160	34.52	1.90	69.71	28.6	2.02	89.0
18	10	30	50	140	42.82	3.58	65.64	23.5	2.50	83.0
19	15	24	50	140	50.25	3.60	68.00	28	4.80	82.0
20	10	30	50	140	42.84	3.50	66.41	24	2.20	80.0
21	5	36	50	140	27.55	2.00	55.00	28.5	1.66	76.0
22	15	30	35	140	54.87	4.04	62.00	25	4.80	73.0
23	5	30	50	120	25.80	2.35	50.35	30.5	1.76	57.0
24	5	30	65	140	24.00	1.60	56.80	28.6	2.32	79.0
25	15	30	65	140	50.3	3.58	69.00	27.4	4.84	79.0
26	10	30	35	160	44.18	1.92	63.11	23.2	2.23	89.0
27	15	36	50	140	56.32	3.50	67.88	30	4.50	80.0

Mean of two trials done at each set of experimental conditions.

the response decreases with increasing input when the parameter estimate is negative. The statistical analysis of variance (ANOVA) was carried out to determine the significance and impact of each main factor as well as their interactions on their response. Numerical output of ANOVA includes F value which provided a means of ranking variables relative to one another and the statistical significance is shown as a p value $<$ 0.05.

Microparticle Characterization

Particle Morphology Morphology of the microparticles was examined by scanning electron microscopy (QUANTA 200 FEI). Dry particles were attached to specimen stubs using double sided tape and excess particles were blown out using a capillary tube. Microparticles were imaged using a 5 kV accelerating voltage, 10 mm working distance and emission current of 348 μA by scanning fields randomly at several suitable magnifications.

Fourier Transform Infrared Spectroscopy (FTIR)

Infrared spectra of drug, excipients and drug-excipient blends were recorded on a FTIR spectrophotometer (Shimadzu 8400S, Kyoto, Japan). A mini press potassium bromide disk was used to prepare a transparent disk of samples. Background spectrum was collected before running each sample. The samples were analyzed between wavenumbers 4000 and 400 cm^{-1}. IR solution 1.10 software (Shimadzu, Kyoto, Japan) was used for the analysis of the FTIR spectra and for recording the data from the spectra. The major and important peaks were reported in cm^{-1}.

Determination of Yield The yields of the microparticle were calculated as the percentage of the ratio of weight of recovered spray dried powder ($W_{recovered}$) to the total amount of dry solids in the initial feed solution (W_{total}).

$$\text{Yield}=\frac{W_{\text{recovered}}}{W_{\text{total}}}\times 100 \quad (2)$$

Determination of Moisture Content The moisture content of the spray dried microparticles was determined by the oven drying method. Accurately weighed samples were placed in a hot air oven (Adair Dutt and Co. Ltd., Calcutta, India) heated at 102°C and weighed on an analytical balance (Citizen Scale Pvt. Ltd., Delhi, India) until constant mass. Average of three weight loss measurements was recorded.

Determination of Drug Entrapment Efficiency Accurately weighed quantity of microparticles (20 mg) was dissolved in 0.1 N HCl. The microparticles were magnetically stirred to promote swelling and complete dissolution of the polymer. The obtained solution was filtered through a 0.45 μm syringe filter. The amount of DX was analysed by ultraviolet spectroscopy at a wavelength of 271.6 nm against calibration curve. The drug entrapment efficiency (EE) was calculated using the following equation:

$$\text{EE}=\frac{A_{\text{actual}}}{A_{\text{loading}}}\times 100 \quad (3)$$

where, A_{actual} is the actual amount of the drug encapsulated and A_{loading} is the amount of drug loading calculated from the amount of drug added during the manufacturing process. All the experiments were carried out in triplicate.

Determination of Carr's Index The bulk density (ρ_b) and tapped density (ρ_t) values were used to calculate the Carr's compressibility indices (CI) according to the following equation:

$$\text{CI}=\left(\frac{\rho_t-\rho_b}{\rho_t}\right)\times 100 \quad (4)$$

Bulk density (ρ_b) of microparticles was assessed by filling dry microparticles into a 5 ml graduated cylinder and the top was levelled. The weight (W) and volume (V_b) occupied by the powder was recorded.

$$\rho_b=\frac{W}{V_b} \quad (5)$$

The tap density (ρ_t) of the spray dried powders was then evaluated by tapping the cylinder onto a level surface at a height of about 2 cm, until no change in volume is observed. The resultant volume was recorded as V_t.

$$\rho_t=\frac{W}{V_t} \quad (6)$$

Each measurement was carried out in triplicate.

Determination of Microparticle Aerodynamic Diameter The aerosol performance of a particle largely depends on its aerodynamic diameter, a parameter which is based on the particle size and density. The particle size of the microparticles was determined using an optical microscopy method. Approximately 100 microparticles were taken on a glass slide and particle size measured using a calibrated optical microscope (Olympus OIC, Tokyo, Japan) equipped under regular polarized light. The theoretical aerodynamic diameter (D_{aero}) can be expressed as follows:

$$\text{d}_{\text{aero}}=\left(\sqrt{\frac{\rho_t}{\rho_1}}\right)\times d \quad (7)$$

where, $\rho_1=1$ g/cm^3.[19]

Optimization Data Analysis and Validation of Optimization Model In this study, a collective level of formulation variables and spray drying condition (as input variable settings) was required to produce DX loaded microparticles with desirable physicochemical properties (i.e., the highest yield, lowest moisture content, high entrapment efficiency and low aerodynamic diameter). Each of the processing variables was important in determining the quality of the finished product, while the optimal settings of design variables for an individual response might be far from the optimal area for another response. Thus, those properties should be considered together for a multiple optimization process. The final optimum experimental parameters were calculated using the Minitab Response Surface Optimiser function, which allows for compromise among the various responses. This function helps in determining the exact optimum level of independent variables leading to individual and overall response goals. The optimisation was accomplished by obtaining the individual 'desirability' (d) for each response, combining the individual desirabilities to obtain the composite desirability (D), and finally by maximising the composite desirability and identifying the optimal factor settings. The measured responses are transformed to a dimensionless desirability (d) scale. The scale of the desirability function ranges between $d=0$, for a completely undesirable response, to $d=1$ for a fully desired response above which further improvements would have no importance. This measure of the composite desirability is the weighted geometric average of the individual desirabilities or the responses.

For method validation, the experimental data were compared with predicted values in order to verify the adequacy of the final reduced models.

Differential Scanning Calorimetry The thermal response of pure drug and optimised formulation was analyzed using a differential scanning calorimeter (DSC, Model DSC-60, Japan). The instrument was calibrated using indium standards. Samples (~3–5 mg) were hermetically crimp sealed in flat bottom aluminium pans and heated from 30 to 300℃ at the rate of 10℃/min under an atmosphere of nitrogen.

Determination of Microparticle Aerodynamics The aerodynamic properties of the optimised batch of microparticles were determined using an eight stage, nonviable Andersen cascade impactor (ACI) with a preseparator (Graseby-Andersen, Atlanta, GA, USA). A hard gelatin capsule (size no. 2, Universal capsules, Mumbai, India) previously stored in a dessicator for at least two days, was manually loaded to approximately 50% of its volume with the microparticles and placed in a monodose inhaler (Miat S.p.a Milan, Italy). For each actuation (4s), capsule was pierced and the liberated powder was drawn through the impactor operated at a continuous air flow rate of 60 l/min (produced by a vacuum pump connected to the outlet of the ACI). After 15 actuations for one determination, the amount of microparticles deposited in the device, throat, preseparator and each stage of ACI was collected. Under these conditions, the effective cut off diameters were 8.6, 6.5, 4.4, 3.3, 2.0, 1.1, 0.54 and 0.25 μm for stages 0–7, respectively.

The recovered dose was defined as the total amount of drug recovered per capsules after each actuation. Emitted dose was determined as the percent of total powder mass exiting the capsule (i.e., from throat to filter in the ACI). The fine particle fraction (FPF) was defined as the fraction of drug less than 5.0 μm. The mass median aerodynamic diameter (MMAD) of the microparticles was determined from the plot of inverse cumulative mass percentage undersize in each stage against the log effective cut off diameter of the respective stages. Geometric Standard Deviation (GSD) is a measure of the spread of an aerodynamic particle size distribution. It was calculated as the ratio of diameters at which 84% and 16% of the aerosol mass are contained.

Determination of *In Vitro* Drug Release *In vitro* release of DX (in triplicate) from the optimised batch of microparticles (equivalent to 10 mg DX) was studied by dialysis bag diffusion technique. The dialysis membrane (Sigma, thickness 0.025 mm, mol. wt. cutoff 6000–8000 Dalton) was cut into equal pieces (6 cm×2.5 cm) and soaked in distilled water for 12 h before use. Accurately weighed quantity of microparticles (equivalent to 10 mg DX) was suspended in 5 ml of phosphate buffer saline (PBS) pH7.4 and placed in the dialysis pouch with the two ends fixed by thread. The pouch was attached to the paddles of USP type II dissolution tester (Electrolab, TDT 06P model) and put into the flask containing 500 ml of PBS, maintained at 37±0.2℃ and stirred at 50 rpm. Aliquot samples were withdrawn at regular time intervals (and fresh PBS replaced) and analyzed by UV spectrophotometer as described earlier.

Statistical Analysis Analyses of variance test (ANOVA) (Minitab 16, Minitab Ltd., Coventry, UK) was used to study the significance and adequacy of the regression model. The statistical significance of the second order model equation was determined from Fisher variance ratio (F value), lack of fit and the multiple coefficient of determination (R^2) and p values of <0.05 were considered to be significant.

RESULTS AND DISCUSSION

Morphology The overall shape of the particles was found to be spherical like doughnuts in the size range of 1.16–5.2 μm. The SEM images also indicated that the powders are amorphous in nature. The particle morphology was found to depend on feed composition and spray drying condition as shown in Fig. 1.

The particle surface varied from smooth (Fig. 1 (a)) to wrinkled texture (Fig. 1(b)). The wrinkled morphology is formed by uneven shrinkage forces during the drying of droplets, depending on the feed composition and process conditions. Images of burst particles were also seen under extreme conditions (Fig. 1(c)).

FTIR FT-IR spectral pattern of DX shows multiple sharp peaks between 1600 and 1400 cm^{-1} corresponding to aromatic C=C bonds, peak at 1242 cm^{-1} corresponding to C-O bond. Characteristic peaks at 3400 and 3200 cm^{-1} corresponding to primary OH and primary NH, respectively were also seen. Although the intensity of DX bands is low due to the low weight ratio of DX in the physical mixture, they were well preserved as shown in Fig. 2. These results indicate no or minor interaction between drug and excipients.

Yield The yield of dry powders was found to vary widely, from 20.62 to 56.32% of the initial dry

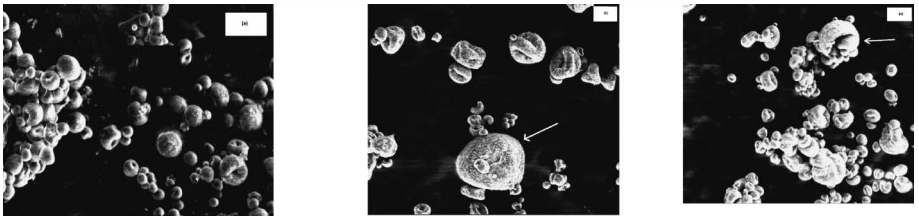

Fig. 1. S.E.M. Photomicrographs of the Antibiotic Loaded Microparticles Produced by Spray Drying with Different Feed Compositions

(a) Typical spherical morphology of the majority of microparticles. (b) Microparticles with wrinkled morphology (Run 8). (c) Burst microparticles (Run 13). 5000× magnification (Scale=20 μm).

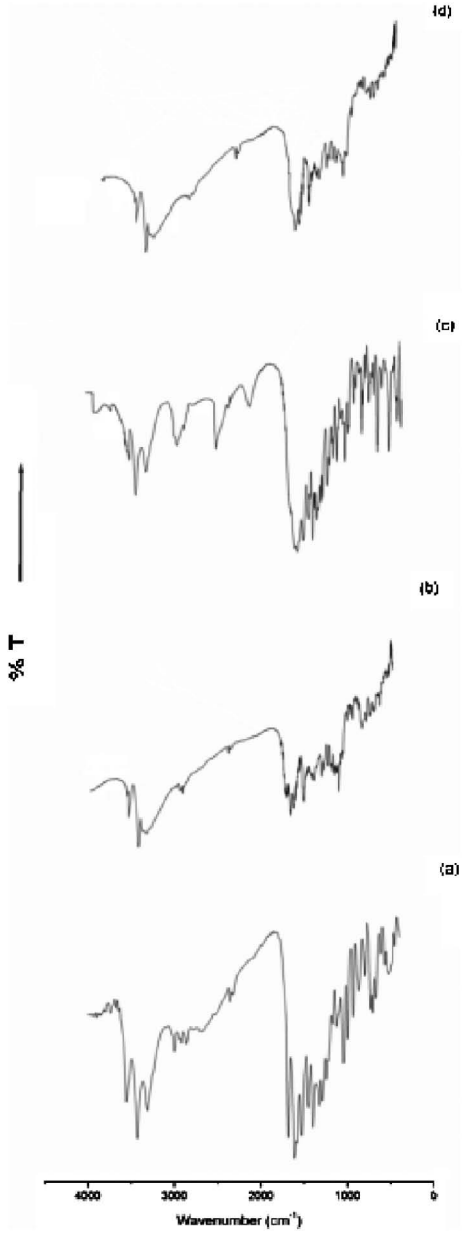

Fig. 2. FTIR Spectra of (a) Pure DX and Physical Mixture of (b) DX and Lactose (c) DX and Leucine and (d) DX and SC

solids taken in the feed solution. The yield was lowest in case of run 9 while the highest yield was observed in case of run 27. In general, yield was found to depend primarily on the feed composition. Most of the experimental runs resulted in less than 45% yield because of the difficulties in collection of small particles. Powders adhering to the walls of cyclone and drying chamber resulted in loss of powder yield. Also, some of the smaller and lighter particles were exhausted by the aspirator.

A model was fit for yield as a function of the input variables (Table 2). The main effects of polymer concentration ($F=5.15$, $p<0.05$), leucine concentration ($F=9.78$, $p<0.01$), ethanol concentration ($F=15.77$, $p<0.01$) and inlet temperature ($F=6.45$, $p<0.05$) on yield of the spray dried powder were found to be significant. An increase in polymer concentration from 5 to 15% w/v resulted in formation of denser particles which increased deposition of particles in collection chamber via the cyclone. The increase in yield due to high ethanol concentration can be attributed to rapid phase separation and solidification on drying. In general, the yield of the spray drying process improved with increased leucine content in the initial feed solution. Leucine decreases the interparticulate cohesive interactions responsible for low yield. This may be attributed to its interference with the weak van der Waal' s and coulombic bonding forces, between the small particles which help to keep the particles separated.[20] The negative quadratic effects indicate that higher amount of leucine and ethanol in the feed composition can be detrimental to this increase in yield. The interaction of inlet temperature and ethanol concentration is shown in Fig. 3. It was observed that greater than 40% yield could be achieved by increasing the inlet temperature above 130°C while keeping the ethanol concentration below 50% v/v in the feed.

Table 2. Estimated Regression Coefficients for Response Parameters

Term	Yield (%)		Moisture content (%)		EE (%)		Carr's index		d_{aero} (μm)		Outlet temp. (℃)	
	Coefficient	F	Coefficient	F	Coefficient	F	Coefficient	F	Coefficient	F	Coefficient	F
Constant	−210.529	—	−33.3482	—	31.5539	—	232.102	—	17.6397	—	−393.979	—
X_1	3.410*	5.15	0.8293**	12.01	6.9047***	40.43	−2.902*	5.55	0.3013	2.16	9.327*	7.15
X_2	4.685**	9.78	0.5433*	5.19	−2.5376*	5.49	−12.204***	98.87	−0.2322	1.29	2.799	0.65
X_3	2.129**	15.77	0.0814	0.91	0.6194	2.55	−0.384	0.76	−0.1196	2.67	2.992*	5.78
X_4	1.323*	6.45	0.3577***	18.58	0.0816	0.05	0.308	0.52	−0.1594*	5.02	3.754**	9.63
X_1^2	−0.026	0.94	−0.0139**	10.91	−0.1960***	105.79	1.088**	16.47	0.0291***	65.31	−0.100	2.67
X_2^2	−0.055*	8.96	−0.0046	2.48	0.0289*	4.77	0.172***	131.43	0.0038	2.33	−0.020	0.23
X_3^2	−0.009*	8.55	−0.0008	3.08	−0.0048*	5.10	0.008**	10.10	0.0010*	5.70	−0.014	4.2
X_4^2	−0.003	3.05	−0.0011	3.82	0.0008*	0.51	−0.001	0.15	0.0002	0.52	−0.008	4.31
$X_1 \times X_2$	−0.007	0.08	0.0008	0.04	0.0034	0.03	0.119***	32.86	−0.0052	2.22	−0.042	0.50
$X_1 \times X_3$	−0.014	1.93	−0.0002	0.02	0.0067	0.83	0.008	0.85	−0.0023	2.67	0.000	0.00
$X_1 \times X_4$	0.006	0.65	−0.0029*	5.53	−0.0159*	8.33	0.023**	13.9	0.0023*	4.90	−0.042*	5.65
$X_2 \times X_3$	−0.002	0.09	−0.0002	0.02	0.0099	2.60	0.000	0.00	0.0001	0.00	−0.017	0.72
$X_2 \times X_4$	−0.005	0.59	−0.0019	3.60	0.0016	0.12	0.001	0.06	0.0036***	17.11	−0.002	0.02
$X_3 \times X_4$	−0.009**	11.51	−0.0000	0.00	−0.0023	1.55	−0.003	2.32	0.0004	1.33	−0.007	1.59

X_1=Polymer concentration (% w/v), X_2=Leucine concentration (% w/v), X_3=Ethanol concentration (% v/v), X_4=Inlet temperature (℃). Student t test statistic; '—'=not calculated, *=significant, **=very significant, ***=highly significant.

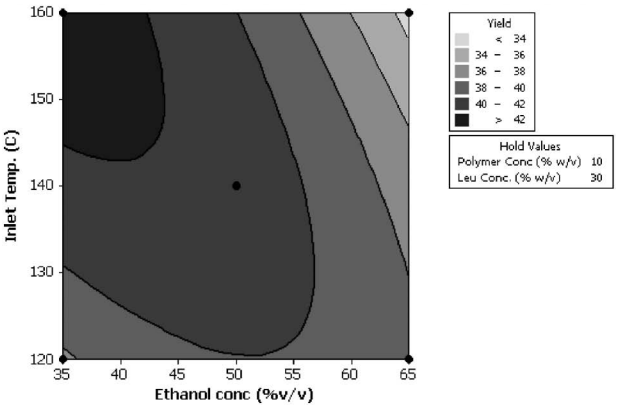

Fig. 3. Response Contour Plot Showing the Combined Effect of Ethanol Concentration and Inlet Temperature on Yield

Moisture Content In the spray drying process, solvent evaporation from the atomized liquid droplet takes place instantaneously (less than 25 s). In this short time period, particles fail to achieve equilibrium moisture content as seen in case of methods requiring long drying period. The effects of the independent variables on moisture content of spray dried powders are presented in Table 1. The moisture content in the spray dried powders varied between 1.48 and 4.5%. It is highly dependent on the inlet temperature (F= 18.58) which in turn alters the temperature of the drying air and outlet temperature of the spray dryer. The negative coefficient of inlet temperature indicates that the moisture content decreases linearly with the increase in inlet temperature from 120 to 160℃. The results (Table 1) also indicate that polymer concentration has a significant effect on the microparticle moisture level (F=12.01, $p<0.01$). High levels of moisture content at 15% w/v SC concentration are associated with powder tackiness, agglomeration tendency and poor flow characteristics. This may be attributed to the ability of SC to retain water in the microparticle during spray drying. The amount of leucine in the feed solution also influenced the moisture content in the spray dried powders (F= 5.19, $p<0.05$). It may be due to the hydrophobicity of leucine. The interaction between polymer concentration and inlet temperature was found to be significant (F=5.53, $p<0.5$).

As shown in Fig. 4, less than 3% moisture content could be obtained at an inlet temperature above 140 and 145℃ for 10% w/v and 15% w/v SC concentration, respectively. At the lowest SC concentration (5 % w/v), the moisture content was found to be less than 2.5% below 145℃.

Encapsulation Efficiency Encapsulation efficiencies calculated from actual drug loadings were found to be high, lying between 50.35 and 69.00% (Table 1). These differences in drug encapsulation can be explained in terms of theory of microparticle formation.[21] The encapsulation of drugs into poly-

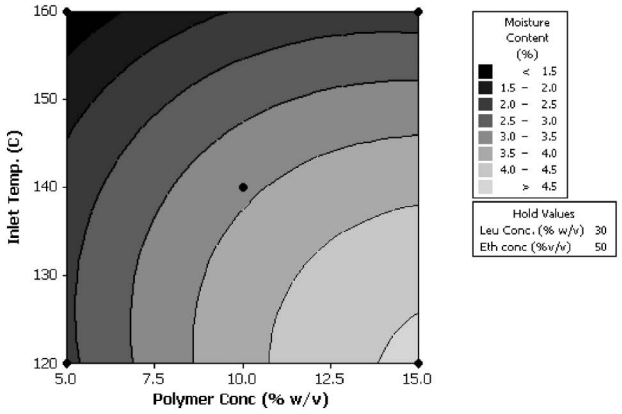

Fig. 4. Response Contour Plot Showing the Combined Effect of Polymer Concentration and Inlet Temperature on Moisture Content

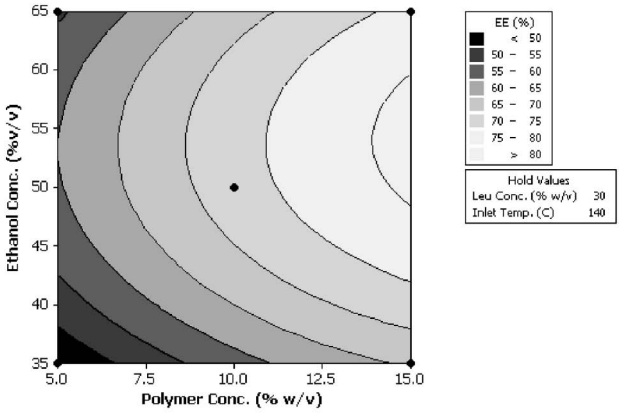

Fig. 5. Response Contour Plot Showing the Combined Effect of Polymer Concentration and Ethanol Concentration on Encapsulation Efficiency (EE)

meric particles by spray drying depends on the time taken by the evaporating droplet to shrink and subsequent arrangement of solute at the surface and centre.

The coefficients for the polynomial equation relating the response and independent variables are shown in Table 2. The predicted values and the experimental values were in excellent agreement with a correlation of $R^2=98.14\%$. The coefficients reflect that polymer concentration showed the highest influence on the encapsulation efficiency ($F=40.43$, $p<0.001$). Leucine concentration also influenced the encapsulation efficiency ($F=5.49$, $p<0.05$). Polymer concentration ($p<0.001$), leucine concentration ($p=0.05$) and ethanol concentration ($p<0.05$) exhibited non-linear (quadratic) effects on drug encapsulation. This indicates that only at higher levels the EE decreases with polymer and ethanol concentration while an increase in EE can be seen with ethanol concentration and inlet temperature. As shown in Table 2, there is significant interaction between polymer concentration and inlet temperatures on encapsulation efficiency ($p<0.5$). From Fig. 5, it is evident that on increasing the concentration of SC beyond 10% w/v, encapsulation efficiency greater than 64% can be achieved irrespective of the spray drier inlet temperature (120–160°C). However, greater than 68% encapsulation efficiency can be achieved when SC concentration is within 10–15% w/v at temperatures above 150°C. When the SC concentration is high (10 to 15% w/v), precipitation of polymer increases which limits the drug diffusion across the phase boundary. Fast polymer solidification at high temperature (above 150°C) resulted in high encapsulation efficiency.

Carr's Index All the spray dried powders have similar bulk density (0.32 to 0.42 mg/ml). However, their tapped density is different and ranges from 0.26 mg/ml to 0.44 mg/ml. Previous investigators have reported that tapped density directly influences the aerodynamic nature of the particles.[22] Carr's Index values of less than 25 are usually taken to indicate good flow characteristics, whereas values above 40 indicate poor powder flowability. High Carr's compressibility index also reveals the cohesive nature of the particles. In general, the results suggest that the acceptable flowability of prepared spray dried particles could be attained by varying the feed composition and inlet temperature (Table 1).

The coefficient of main effect of leucine concentration was highest ($F=98.87$) and positive. The amount of leucine significantly improves the flow properties of the powders ($p<0.001$) by increasing the bulk of the powders. The interactions between particulates in a less tightly packed system are reduced thereby enhancing powder flow properties.[23] The quadratic effect of polymer concentration was found to be significant ($F=16.47$, $p<0.01$). Increase in feed viscosity associated with high polymer concentration resulted in denser particles. These dense particles exhibit good flow properties. Interaction between polymeric concentration and leucine concentration was found to be highly significant ($F=32.86$, $p<0.001$). As shown in Fig. 6(a), the Carr's index decreases with the increase in leucine and polymer concentration. Complex interaction of inlet temperature and polymer concentration is shown in Fig. 6 (b). Less than 25% carr's index was observed when

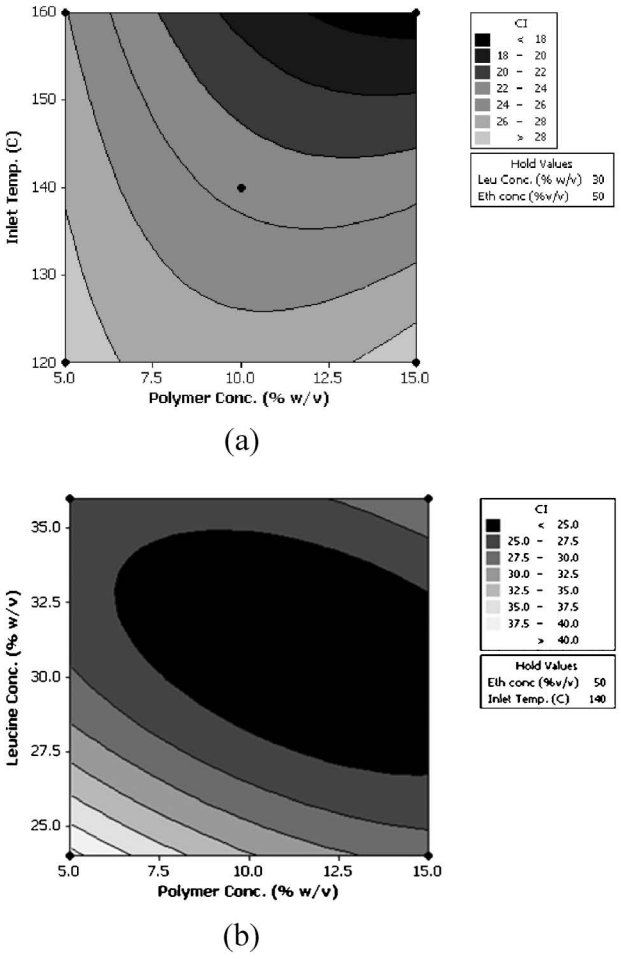

Fig. 6. Response Contour Plot Showing the Combined Effect (a) Polymer concentration and inlet temperature and (b) Polymer concentration and leucine concentration on Carr's index (CI).

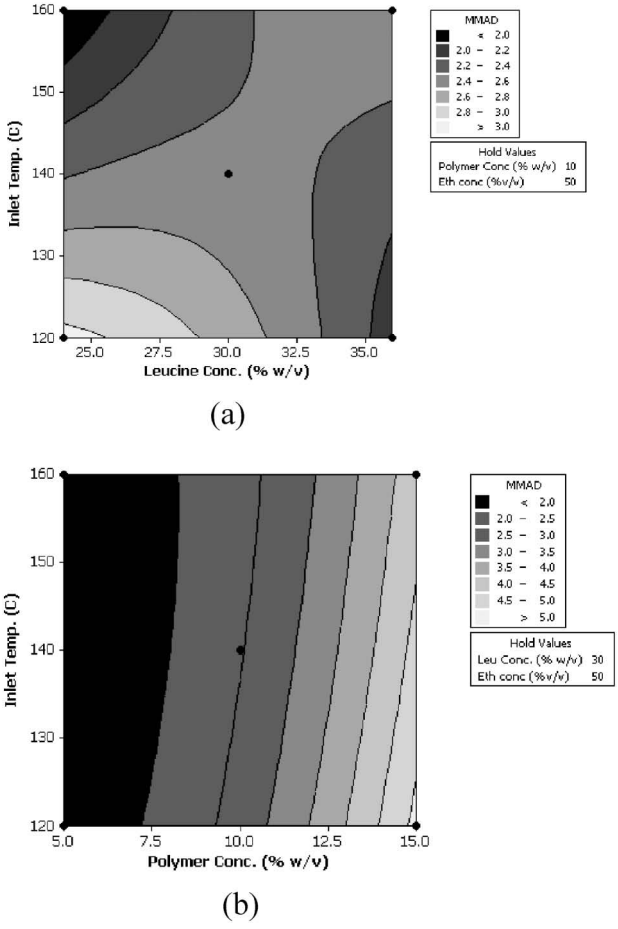

Fig. 7. Response Contour Plot Showing the Combined Effect (a) Leucine concentration and inlet temperature and (b) Polymer concentration and inlet temperature on aerodynamic diameter (Daero).

the inlet temperature was above 140°C. High polymer concentration is often associated with high moisture content at lower levels of inlet temperature thus, impairing the flow properties of spray dried powders (Carr's index greater than 28%).

Aerodynamic Diameter The aerodynamic diameter of the prepared microparticles was between 1.60 and 5.0 μm. This indicates that powders of respirable size range could be produced by spray drying. Particles less than 3 μm are suitable for deep lung deposition. The main effect of inlet temperature was found to be significant ($F=5.02$, $p<0.05$). The effects of the proportion of formulation components in the feed solution on aerodynamic diameter of spray dried powders were also studied (Table 1). The effect of interaction between leucine concentration and inlet temperature was found to be highly significant ($F=17.11$, $p=0.001$). As shown in Fig. 7(a), complex interactions of leucine concentration and inlet temperature can be seen on d_{aero}. Leucine possesses surfactant properties and thus migrates to the air water interface. At the surface of the droplet, it inhibits the diffusion of solvent vapour resulting in expansion of particle surface.[24] The amount of solvent vapour plays a crucial role and is directly related to the inlet temperature. The surface layer collapses when the vapour pressure is high resulting in the formation of spherical wrinkled doughnut shaped particles (Fig. 1 (b)). This shape limits the point to point contact between particles and hence lowers the d_{aero}. Quadratic effect of polymer concentration was highest ($F=65.31$, $p<0.001$). However, the leucine concentration showed no significant linear or quadratic effect on d_{aero} ($p>0.05$). It was observed that at 36% w/v leucine concentration, charged particles were developed. A positive interaction of polymer concentration and inlet temperature ($F=4.9$, $p<0.05$) was observed in case of d_{aero} (Fig. 7(b)). This can be attributed to the

changes in droplet size exiting the spray nozzle. Viscous solutions at higher concentration of SC and high temperature resulted in higher particle size.

Outlet Temperature A model was developed for outlet temperature which plays an important role in the quality of spray dried microparticles. It is the maximal temperature of drying air mixed with the solvent vapours and dry particles before entering the cyclone. If the outlet temperature is too low, sticky particles are formed in the drying chamber which will not dry completely in the time allowed. The outlet temperature is however not the temperature of the recovered particles.

The result of the model fit for outlet temperature ($R^2=0.94$) is presented in Table 2. The inlet temperature was found to have the most influence on outlet temperature ($F=9.63$, $p<0.01$), followed by the polymer concentration ($F=7.15$, $p<0.05$). The ethanol concentration had a minor ($F=5.78$, $p<0.05$) but significant effect ($p<0.05$) while leucine concentration had no effect on the outlet temperature ($p>0.05$). In general, the outlet temperature increased with rise in inlet temperature and ethanol concentration while it decreased with increase in polymer concentration (Fig. 8). High inlet temperature increases the energy available for the drying process resulting in increase of the outlet air temperature. With the increase in polymer concentration from 5 to 15%, the feed solution forms larger viscous droplets. This is associated with increased heat absorption and consequently quicker heat-mass transfer takes place, reducing the outlet temperature. An increase in the ethanol concentration of the feed solution increases the thermal efficiency of the system. It is likely that some amount of solvent may be trapped at an outlet temperature of 57℃. But, with the increase in the outlet temperature particles burst due to evaporation of the residual solvent. This is evident from Fig. 1(c) which shows inflated particles which are hollow.

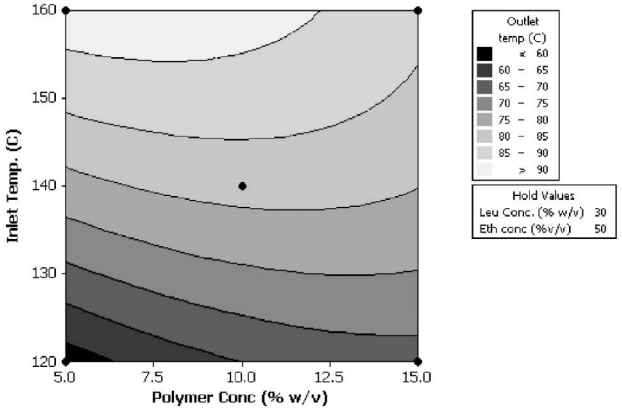

Fig. 8. Response Contour Plot Showing the Combined Effect of Polymer Concentration and Inlet Temperature on Outlet Temperature

Optimization Calculations A numerical optimization technique using the desirability approach was employed to develop a new formulation (DXSC) with the desired responses. The optimization was aimed at maximising yield and EE while minimizing aerodynamic diameter, moisture content, Carr's index and outlet temperature for the new formulation. The composite desirability (D) for the optimal solution was determined to be 0.9090. The optimal calculated parameters were: SC concentration 14.12% w/v, leucine concentration 33.019% w/v, ethanol concentration 36% v/v and inlet temperature 137.64℃. Based on these calculations, the following experimental parameters were set as the optimum: SC concentration 14% w/v, leucine concentration 33% w/v, ethanol concentration 36% v/v and inlet temperature 140℃. For validation of BBD results, the experimental values of the responses were compared with that of the predicted values as shown in Table 3. The observed (mean of 3 trials) and predicted values of response were in close agreement.

X-ray Diffraction Figure 9 shows the XRD pattern of drug (DX) only and drug loaded microparticles. The XRD pattern for DX shows angular ranges and d spacing of 10.98° and 24.43° 2θ at 8.051 and 3.641 Å, respectively. The absence of crystallinity in the DXSC spray dried microparticles was evident from the lack of peaks in the XRD (Fig. 9(b)). This amorphous halo in the XRD pattern is in contrast to the distinctive peaked pattern obtained for the crys-

Table 3. Experimental and Predicted Results for Optimized Microparticle (DXSC)

Response	Observed value	Predicted value (d)	Error (%)
Yield (%)	56.69	54.42 (1.00)	−4.17
Moisture content (%)	3.86	3.97 (0.63)	2.77
EE (%)	61.74	62.89 (0.85)	1.83
d_{aero} (μm)	3.11	3.00 (0.91)	−3.67
Carr's index (%)	23.5	23 (0.91)	−2.17
Outlet temperature (℃)	77.0	75.8 (0.96)	−1.58

d=desirability.

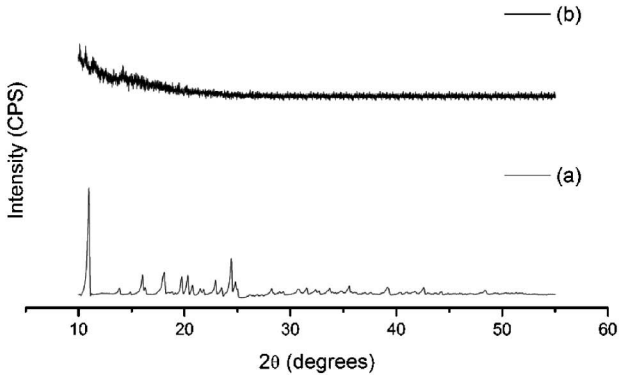

Fig. 9. XRD Spectra of (a) DX and (b) Drug Loaded Microparticles (DXSC)

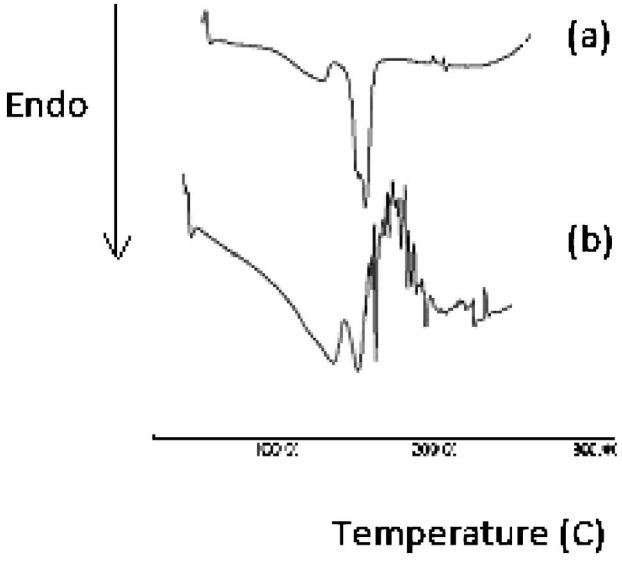

Fig. 10. DSC Thermograms of (a) DX and (b) Drug Loaded Microparticles (DXSC)

talline DX only sample (Fig. 9(a)).

Differential Scanning Calorimetry The physico-chemical characterisation of microparticles was performed by DSC analysis. The DSC thermograms of pure drug (DX) and DX loaded microparticles are shown in Fig. 10. Pure DX showed a complex transition and a large endothermic peak due to the melting of the drug at 168.3°C, followed by a series of 2 small exothermic peaks of crystallization at around 220°C. Two broad endothermic peaks were observed at approximately 150°C in case of DXSC. This may be attributed to glass transition followed by a peak of crystallisation.[25] This suggests the presence of solid dispersion of the amorphous drug in the polymer matrix.

***In Vitro* Powder Aerosolisation** The *in vitro* aerosol deposition of the optimized batch DXSC microparticles was analyzed in an ACI. The recovered dose and emitted doses was found to be 90.9% and 82.75%, respectively, indicating that a majority of the spray dried particles was dispersed from the device. As shown in Fig. 11, less than 20% of the microparticles were deposited in the preseparator. Beyond preseparator, the deposition of microparticles was primarily in the stage 3. The FPF consisted of microparticles less than 5 μm in size. Although, the SEM images revealed that the majority of the particles were in the respirable size range (1–5 μm), the FPF was found to be 49.3%. The mean MMAD was found to be 4.89 μm and GSD was 1.83. It was found to be slightly greater than the theoretical aerodynamic diameter. This may be attributed to the fact that individual particles behave as aggregates.

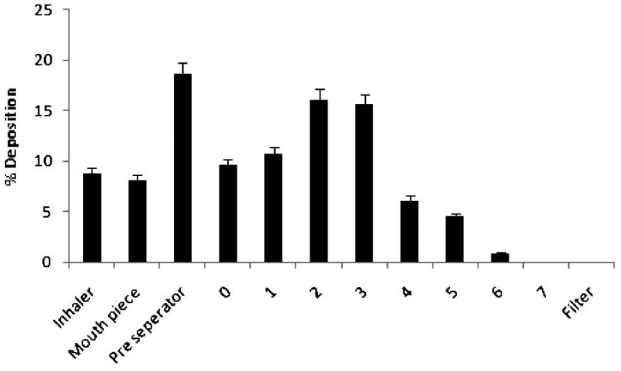

Fig. 11. Deposition Profile for Drug Loaded Microparticles (DXSC) Showing Percent Microparticles Deposited (as percentage of total emitted dose) on Each Stage of ACI

***In Vitro* Drug Release** The *in vitro* release profile of DX from the optimised batch of drug loaded microparticles (DXSC) was compared with drug release from pure drug and results are presented in Fig. 12. As expected, the dissolution of pure drug was rapid and resulted in nearly 100% DX release in approximately 4 h. However, drug release from microparticles had to overcome a barrier of gel diffusion layer which is formed when the dry hydrophilic polymer swells on coming in contact with the physiological fluid. The spray dried microparticles exhibited sustained release characteristics. Initially, nearly 21.05% of the drug was released within 30 minutes of dissolution study. Less than 50% of the drug was released in 8 h of dissolution study. At the end of 24 h, greater than 72% of the drug was released in the above mentioned batches

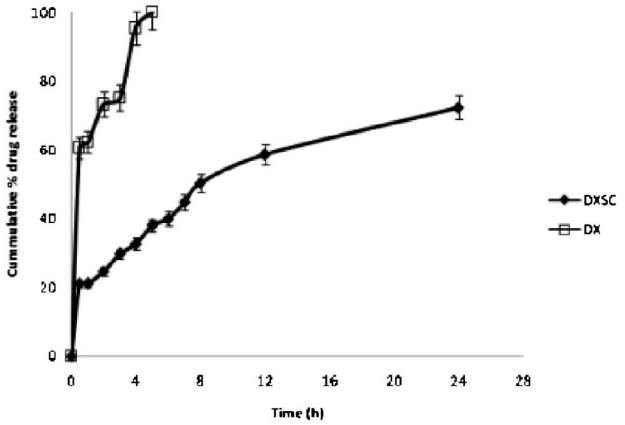

Fig. 12. Comparative *In Vitro* Drug Release Profile of Drug Loaded Microparticles (DXSC) and Pure Drug Solution

To analyse the mechanism and kinetics of drug release, the dissolution profiles were modelled for correlation to Peppas equation for the first 8 h only. The Peppas equation can be described as follows:

$$\frac{M_t}{M_\infty}=kt^n \qquad (8)$$

where, M_t/M_∞ is the fraction of drug release. Using the least squares procedure, the values of n (diffusion exponent), k (kinetic constant) and r^2 (correlation coefficient) were estimated. In spherical matrices, if $n \leq 0.43$, a Fickian diffusion (case-I), $0.4 \leq n < 0.85$, anomalous or non-Fickian transport and $n \geq 0.85$, a case-II transport (zero order) drug release mechanism dominates. The n value for the optimised batches was found to be 0.417 ($r^2=0.965$) indicating Fickian type of drug diffusion ($k=0.417\ h^{-0.417}$).

CONCLUSION

In this study, SC based microparticles for inhalation delivery of DX was prepared by spray drying method. The formation of microparticles was confirmed from the SEM photomicrographs. The FTIR studies revealed no drug excipient interaction. Box-Behnken design was used to study the influence of various independent variables on microparticle characteristics. It was observed that on increasing the concentration of this hydrophilic polymer, the viscosity of the feed solution is enhanced resulting in the formation of larger, denser particles with higher moisture content. On the other hand, leucine being hydrophobic with surfactant like properties results in the formation of wrinkled particles which decreases the interparticulate cohesive forces at lower levels, increases yield, improves flowability but decreases moisture content and theoretical aerodynamic diameter. The thermal efficiency of the system increased with ethanol concentration resulting in rapid phase separation and solidification of particles. Changes in the inlet temperature settings causes difference in the energy available for drying. Significant interactions of inlet temperature with other input variables were also observed. The quantitative effect of these factors at different levels was predicted by using polynomial equations.

The optimization of these formulation and process variables was aimed at maximising yield and EE while minimizing aerodynamic diameter, moisture content, Carr's index and outlet temperature for the new formulation. The optimized formulation was prepared using SC concentration 14% w/v, leucine concentration 33% w/v and ethanol concentration 36% v/v at an inlet temperature of 140°C. The optimized batch (DXSC) prepared by using these predicted levels of factors provided desired observed responses forming microparticles with yield 56.69%, moisture content 3.86%, EE 61.74%, d_{aero} 3.11 μm, Carr's index 23.5 % and outlet temperature 77°C. Further, solid state characterization of DXSC by XRD and DSC confirmed that drug was dispersed in the SC matrix in the amorphous state. Results of aerosolization assessment of DXSC reveal an acceptable MMAD (4.89 μm) and fine particle fraction (49.3%). The spray dried microparticles exhibited sustained release characteristics and more than 72% drug was released in 24 h. This study demonstrated that SC based microparticles prepared herein can potentially be exploited as carriers for the inhalation delivery of DX.

Acknowledgment First author is thankful to University Grants Commission (UGC), India for providing senior research fellowship.

REFERENCES

1) Wood G. C., Swanson J. M., *Drugs*, **67**, 903–914 (2007).
2) Ei-Sabina D., Price R., Edge S., Young P. M., *Drug Dev. Ind. Pharm.*, **32**, 243–251 (2006).
3) Chan H-K., Clark A. R., Feeley J. C., Kuo M-C., Lehrman S. R., Pikal-Cleland K., Miller D. P., Vehring R., Lechuga-Ballesteros D., *J. Pharm. Sc.*, **93**, 792–804 (2004).
4) Chan H-K., *Colloids and Surfaces A: Phys-*

icochem. Eng. Aspects, **284–285**, 50–55 (2006).
5) Tobyn M., Staniforth J. N., Morton D., Harmer Q., Newton M. E., *Int. J. Pharm.*, **277**, 31–37 (2004).
6) Kuo M-C., Tep V., Lechuga-Ballesteros D., Lalor C., Yang B., Kadrichu N., Clark A., Presented at AAPS Annual Meeting and Exposition, Toronto, Canada, November 2002.
7) Esposito E., Menegatti E., Cortesi R., *Int. J. Pharm.*, **288**, 835–849 (2005).
8) Muttil P., Kaur J., Kumar K., Yadav A. B., Sharma R., Misra A., *Eur. J. Pharm. Sci.*, **32**, 140–150 (2007).
9) Learoyd T. P., Burrows J. L., French E., Seville P. C., *Eur. J. Pharm. Biopharm.*, **68**, 224–234 (2008).
10) Ohashi K., Kabasawa T., Ozeki T., Okada H., *J. Control. Rel.*, **135**, 19–24 (2009).
11) Sakagami M., Sakon K., Kinoshita W., Makino Y., *J. Control. Rel.*, *77*, 117–129 (2001).
12) Westmeier R., Steckel H., Proceedings of Drug Delivery to the Lungs 19 (2008), ⟨http://ddl-conference.org.uk/files/posters/39.Westmeier.pdf⟩ cited 12 January, 2011.
13) Li H-Y., Seville P. C., *Int. J. Pharm.*, **385**, 73–78 (2010).
14) Mishra M., Mishra B., *J. Pharm. Pharmac.*, **58**, 1281–1282 (2010).
15) Mishra B., Sankar C., Mishra M., *J. Drug Target.*, **19**, 204–211 (2011).
16) Holmes N. E., Charles P. G. P., *Clin. Med. Ther.*, **1**, 471–482 (2009).
17) Bendeck M. P., Conte M., Zhang M., Nili N., Strauss B. H., Farwell S. M., *Am. J. Pathol.*, **160**, 1089–1095 (2002).
18) Ragonese R., Macka M., Hughes J., Petocz P., *J. Pharm. Biomed. Anal.*, **27**, 995–1007 (2002).
19) Bosquillon C., Préat V., Vanbever R., *J. Control. Rel.*, **96**, 233–244 (2004).
20) Chougule M. B., Padhi B. K., Jinturkar K. A., Misra A., *Recent Pat. Drug Deliv. Formul.*, **1**, 11–21 (2007).
21) Vehring R., *Pharm. Res.*, **25**, 999–1022 (2008).
22) Bosquillon C., Lombry C., Preát V., Vanbever R., *J. Control. Rel.*, **70**, 329–339 (2001).
23) Lucas P., Anderson K., Potter U. J., Staniforth J. N., *Pharm. Res.*, **16**, 1643–1647 (1999).
24) Wang L., Zhanga Y., Tang X., *Int. J. Pharm.*, **375**, 1–7 (2009).
25) Adi H., Young P. M., Chan H-K., Stewart P., Agus H., Traini D., *J. Pharm. Sci.*, **97**, 3356–3366 (2008).